Journal of Physics: Conference Series **505** (2014) 012038 doi:10.1088/1742-6596/505/1/012038

Positronium cooling at cryogenic temperature for advanced experiments

R S Brusa[1], L Di Noto[1], S Mariazzi[1] and G Nebbia[2]

[1] Dipartimento di Fisica, Università di Trento and TIFPA-INFN, Via Sommarive 14, I-38123 Povo, Trento, Italy
[2] INFN Padova, Via Marzolo , 35131 Padova, Italy

E-mail: brusa@science.unitn.it

Abstract. New Ps spectroscopy measurements, formation of antihydrogen for antimatter-matter comparison experiments, production of Ps beams require the efficient production of cooled positronium in vacuum. At present the most efficient positron-positronium converters are silica based ordered or disordered porous materials, in which formed Ps decreases its kinetic energy by collisional cooling. Recently new positron-positronium converters based on oxidized nanochannels in silicon were found to be very promising because of the tunability of the nanochannel size, which allows to overcome the limits imposed to the Ps cooling by the quantum confinement. With these converters, Ps with temperatures as low as 150 K was detected in vacuum by a TOF apparatus. The Ps formation, quantum confinement, collisional cooling and emission into vacuum from nanochanneled silicon will be discussed in light of recent results.

1. Introduction

Positronium (Ps), the metastable electron-positron bound state, can be formed by injecting a slow positron beam with energy ranging from few eV to some keV in different targets. In metals or semiconductors, Ps is produced at the surface and not in the bulk, where it gives a local enhancement of electron density that prevents a stable binding with a single electron. In insulators Ps can be formed in the bulk and/or at the surface. The basic principles of Ps formation and emission are well described and discussed in the reviews of Ref. 1-3.

In the last years, the availability of intense positron bunches with the Surko trap [4] has allowed Mill's research group to study Ps-Ps interactions [5] finding evidence of positronium molecule (Ps_2) formation [4, 6], to perform Ps_2 optical spectroscopy [7] and Ps excitation in Rydberg states [8].

At present several groups have increased their research efforts at looking both for materials giving high Ps yield and for efficient Ps cooling. In particular, new measurements and experiments demand cooled Ps in vacuum or in closed cavities.

Cold Ps, reducing the Doppler broadening of the Ps atomic transitions, will allow more precise Ps spectroscopy measurements. Indeed, it is also necessary to start with a pre-cooled Ps, at least to 90 K, to make for the first time a Ps laser cooling at the recoil temperature $T_r = 295$ mK [6].

In the AEgIS (Antimatter Experiment: gravity, interferometry, spectroscopy) experiment running at the AD (Antiproton Decelerator) hall at CERN, an antihydrogen ($\bar{H}$) cold beam will be produced by charge exchange between antiprotons and cooled Ps excited in Rydberg states [9, 10]: cold Ps [11] is

essential to increase the cross section of the reaction $\bar{p} + Ps^* \rightarrow \bar{H} + e^-$. The first milestone of AEgIS is the test of the weak equivalence principle of General Relativity by measuring the gravitational interaction between antimatter as $\bar{H}$ and matter.

High yield $e^+ \rightarrow Ps$ converters will make Ps beams feasible. These can be used to fill magnetic traps for positron-electron plasma studies [12]; furthermore, the proposed Ps free fall experiment [13] needs a cold Ps beam. Ps accumulation (at least 10^{18} Ps/cm^3) and cooling in cavities is a step towards the Ps Bose Einstein condensation [4, 6].

The Ps yield in metals and semiconductors can be increased up to 100% by heating the sample above room temperature (RT) and activating the thermal emission of Ps. In this case, positrons trapped at the surface by image charge forces, forms Ps [1-3]. Unfortunately, with these targets there is no way to combine efficient conversion with low Ps kinetic energy (few tens of meV). Recently, another Ps emission channel from clean surface of p and n type Si (111), Si (100) crystals was discovered [14]. Energetic Ps emission ($\langle E_{\perp Ps} \rangle$=160 meV, temperature $T = \frac{\langle E_{\perp Ps} \rangle}{k_B}$ =1860 K, where $E_\perp$ is the component of the kinetic energy perpendicular to the surface of the sample), occurs by an exciton-like surface state, and this emission can be laser induced.

Actually, the most efficient way to obtain cool Ps is to use silica nanostructured materials with disordered pores or ordered cavities with sizes that allow to overcome the temperature limit imposed by the quantum confinement [15]. In silica, up to 80% of implanted e^+ forms Ps [16]. Ps can be emitted into nano-pores or nano-cavities from bulk or surface states. By time of flight (TOF) measurements [17], kinetic energies peaked at 1 eV and 3 eV were attributed to Ps emitted from these two states respectively. Successively, the emitted Ps starts to lose energy by collision with the walls of the cavities, and if these cavities are connected with the surface, Ps can escape into the vacuum with a reduced kinetic energy. In the best cases Ps is emitted after complete thermalization at the sample temperature.

In this paper we will discuss Ps cooling with particular emphasis to Ps formation, diffusion and cooling in ordered oxidized nanochannels in Si [18-20]. In this type of samples, overcoming the limit of Ps confinement, we observed Ps escape into vacuum with a thermal distribution at 150 K ($\langle E_{\perp Ps} \rangle$= k_bT = 13 meV) [20]. Characterization of the samples was carried out with different positron annihilation spectroscopy (PAS) techniques and measurements of Ps velocity with a TOF apparatus.

2. Experimental

2.1. Samples

An electrochemical etching procedure, commonly used to produce porous silicon, was optimized to synthesize single-crystals nanochannels oriented perpendicular to the surfaces in p-type Si (100). Important parameters are the density of the doping atoms (Si resistivity), the etching current and the time of etching in a H_2O-HF-ethanol solution. At last an induced moderate temperature oxidation in air is necessary to form a silica layer on the internal surface of the channels. The silica layer is the region where Ps is formed and emitted into the nanochannels. Typical sample synthesis parameters are reported and discussed in Ref. 18-19. This method allows tuning the size of the nanochannels, extending about 2 μm in depth, from 4-5 nm to 80-100 nm. The size tuning is obtained by iterating the etching-oxidation steps starting in smaller channels; in this way the nanochannels spatial density remains constant. In this paper we will discuss results obtained from samples with 5-8 nm sized nanochannels.

The morphology of the cavity is expected to influence the Ps cooling process. In comparison with ordered straight nanochannels, in porous SiO_2 sol-gel films produced by spin coating of tetraethoxysilane (TEOS) with sacrificial porogens [21- 23], a more or less connected distribution of pores is obtained after curing the samples at 300-400 °C. In some cases holes of smaller diameter interconnect the disorderly distributed quasi-spherical pores [23].

2.2. PAS techniques

Information about Ps formation, pick-off annihilation and diffusion in nano-channelled silicon samples was obtained by 2γ-3γ annihilation ratio spectroscopy (3γ-PAS) at the Trento slow positron beam [24] and by annihilation Lifetime Spectroscopy (LS) at the Pulsed Low Energy Positron System (PLEPS) [25] at the high intense NEutron induced POsitron source MUniCh (NEPOMUC) [26].

2.3. TOF

TOF measurements were done at the Trento slow positron beam [20]. We derived Ps kinetic energy ($E_{\perp Ps}$) measuring the time t between e^+ implantation in the target, determined by detecting the secondary electrons with channeltrons, and *o*-Ps annihilation in flight at a z distance from the target. *o*-Ps annihilation γ-rays were detected with NaI(Tl) detectors behind a 100 mm long lead shield, with a 5 mm slit. Details in Ref. 20. An improved apparatus [27] is now set up at the NEPOMUC facility.

3. Results and discussion

3.1 Positronium yield

Ps formation was obtained by measuring the oPs lifetime reduced by pick-off with PLEPS and three gammas oPs annihilation by 3γ-PAS, in a sample in which the nanochannels were capped with ~30 nm of TiO_2. The intensity oPs lifetime reduced by pick-off and the oPs 3γ annihilation fraction ($F_{3\gamma}(E_+)$) are, above 4 keV e^+ implantation energy E_+ (the nanochannel region), ~ 15 % and ~ 25 %, respectively (see figure 1a).

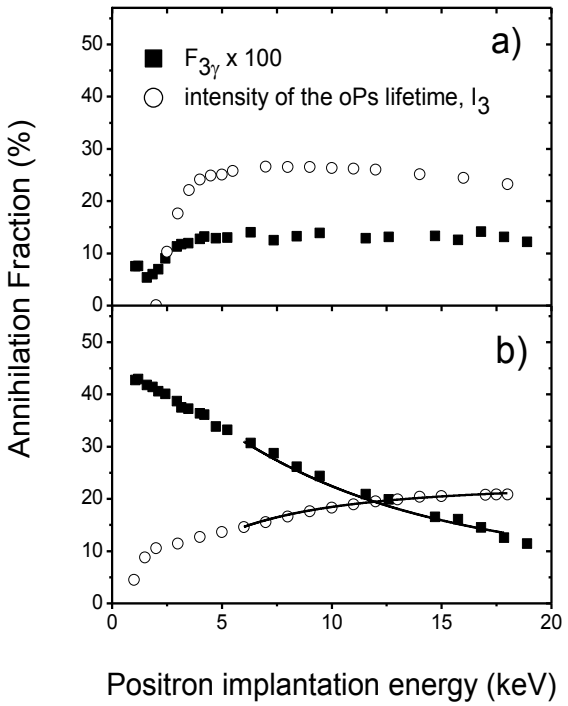

Fig 1: a) intensity I_3 of the oPs reduced lifetime by pick-off (open circles), oPs annihilation into 3 gammas $F_{3\gamma}$ (E_+)x100 (full squares), as measured in 30 nm TiO_2 capped nanochannelled Si sample, as a function of the positron implantation energy; above 4 keV annihilations are into nanochannels. b) Same quantities as in a) but measured in nanochannelled Si sample without capping.

From the lifetime spectra we found that ~ 20 % of implanted e^+ annihilates in Si or as pPs. The remaining ~ 40 % annihilates in the silica layers covering the nanochannels walls and e^+ in surface states with a lifetime of ~400 ps [28]. The low fraction of e^+ annihilating in Si is due to the long e^+ diffusion length (L_+) in Si, about 200 nm, more than ten times the interspacing length among nanochannels. With this L_+ the majority of positrons, after thermalization, reaches the silica layer. Indeed, the efficient production of Ps is caused by the high probability of e^+ reaching the silica layer and the favorable surface/volume ratio in the converter.

3.2 Positronium out-diffusion

Information about the fraction of Ps escaping into vacuum and evaluation of Ps diffusion length L_{Ps} were extracted by analyzing the 3γ-PAS measurements done in an un-capped nanochannelled Si sample. In figure 1b we report the oPs 3γ fraction for the un-capped sample. The shape of the $F_{3\gamma}$ (E_+) curve is characteristic of Ps escaping into the vacuum [18]. At low e^+ implantation energy (< 1 keV), about all Ps (~ 42 %) forms at the outlet of the nanochannels and escapes into vacuum. Increasing E_+, the pick-off annihilation probability increases and the fraction of escaping Ps decreases. Due to the broadening of the positron implantation profile, at higher E_+ (> 15 keV) a fraction of implanted positrons annihilates into Si beyond the end of nanochannels without forming Ps. One should notice that a small fraction of fast escaping Ps at lower E_+ is not detected or detected with lower efficiency, because it annihilates far from the detector view [18]. In the present samples, for E_+ energies higher than ~ 5 keV, a Ps diffusion model can be applied to fit the data [18] because above this energy the diffusion coefficient D_{Ps} has little variations with the implantation depth and can be considered constant. The continuous lines in figure 1b were obtained with a modified model based on rate equations [29] with an unique fitting parameter L_{Ps}. We found L_{Ps} = 721±13 nm corresponding to a D_{Ps}= 0.16 ± 0.01 cm^2/s. The D_{Ps} in nanochannels results to be four to eight times larger than the one found in disordered porous samples. To cool Ps at meV energies, Ps must be formed deeper in the sample, because of the more linear path of Ps escape, due to the straight channels, and the consequent remarkable L_{Ps}

3.3 Positronium cooling

Ps emitted and confined in a cavity decreases its kinetic energy E_{Ps} from 1-3 eV [17] to few meV by collision with the walls of the cavity. Ps interactions with the atoms of the walls and Ps behaviour depend on the Ps energy and on the size *d* of the cavity. Two opposite regimes can be distinguished [3, 15, 23].

If the de Broglie wavelength of Ps is less than *d*, $\lambda_{Ps} = h/\sqrt{4m_0 E_{Ps}} < d$, where m_0 is the e^+ mass, Ps can be treated as a classical particle. This relation requires $E_{Ps} \gg (6\,nm/d)20\,meV$. Up to these energies, Ps collision can be modelled as an elastic scattering between an object of mass $2m_0$ and an atom of mass M of the wall [30, 31].

Differently, when λ_{Ps} becomes comparable to *d*, quantum effects must be taken into account. i) The Ps scattering depends on the overlap of the Ps wavefunction with several atoms of the wall of the cavity. ii) Ps can be quantum confined. For every given size *d*, a minimum Ps energy state exists. In an infinite quantum well (modelling a nanochannel) the minimum energy is $E_{Ps} = h^2/(2m_0 d^2)$ and the corresponding minimum temperature is $T_m = (2E_{Ps})/(3k_b)$ [15].

The nanochannels of the present sample (d = 5-8 nm) were synthetized to reach a minimum temperature $T_m \cong 100\,K$. Figure 2 shows a Ps kinetic energy spectrum, calculated by multiplying a TOF spectrum measured at 150 K sample temperature by t^3. The TOF spectrum was measured at 7 keV positron implantation energy, corresponding to an e^+ mean implantation depth of about $\bar{z}$=500 nm (density of the sample estimated to be 1.9 gcm^{-3}). For the analysis of the TOF spectra we refer to Ref. 20 and reference therein. The best fit to the $E_{\perp Ps}$ spectrum was obtained with the sum of two distributions, a one-dimensional Maxwellian and a beam Maxwellian:

$$\frac{dN}{dE} = A\frac{E_{\perp Ps}{}^{-1/2}}{\sqrt{\pi k_B T_1}} e^{-\frac{E_{\perp Ps}}{k_B T_1}} + B\frac{1}{k_B T_2} e^{-\frac{E_{\perp Ps}}{k_B T_2}}$$

with T_1 = 142±46 K and T_2= 755±43 K.

The above analysis has pointed out the presence of a fraction of Ps that escapes after thermalization with the sample at 150 K. At this temperature this corresponds to a mean escaping energy of $\langle E_{\perp Ps} \rangle$ = k_bT = 13 meV.

Because of the ordered orientation of the nanochannels, the time spent by the Ps atom in the sample before emission (permanence time) is expected to be short compared to the 142 ns oPs lifetime in vacuum and the Ps time of flight. Assuming a simple stochastic approximation for the random walk of a Ps atom bouncing against the wall of the nanochannel and diffusing towards the open end, the number of collision N is related to the path length L and the channel diameter *d* (single step between collisions) by $N=L^2/d^2$. In the diffusion limit $D_{Ps}=L/2\tau$ where τ, is the mean time for Ps to cover L. For Ps, formed implanting e^+ at 7 keV and escaping into vacuum after cooling from nanochannels with *d*=5 nm, we calculate $N=1 \div 2\ 10^4$ and a medium permanence time of τ = 8÷15 ns, considering L in a range between 500 to 700 nm.

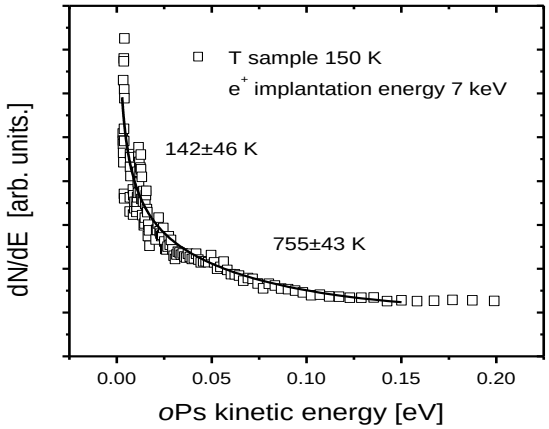

Fig. 2 : Ps kinetic energy spectrum obtained by multiplying by t^3 a TOF spectrum measured at 150 K sample temperature and 7 keV positron implantation energy and 1 cm distance from the target.

4. Conclusions

Oxidized nanochannels in silicon show to be a convenient $e^+ \rightarrow$ cooled Ps converter for performing advanced experiment. The tunability of the nanochannels size allows one to avoid the quantum confinement and to cool Ps down to cryogenic temperature. In the presented case-study, a Ps thermalized fraction is obtained at 150 K. Preliminary measurements have pointed out a fraction of 50 K cooled Ps in a sample with larger nanochannels.

However, the detailed description of the cooling process is far from being completely understood. Ps starts its cooling history as a classical particle then, progressively, its diffusion and its interaction with the surrounding turn into quantum nature. The possibility of studying the Ps cooling and thermalization in different size nanochannels could help understanding the different cooling regimes. Precise direct measurements of the Ps permanence time before escaping into vacuum would be also of extreme interest for checking the validity of cooling models.

Acknowledgments

The Forschungs-Neutronenquelle Heinz Maier-Leibnitz (FRMII) facility is gratefully acknowledged for allocation of beam time at the NEPOMUC facility.

References

[1] Schultz P J and Lynn K G 1988 *Rev. Mod. Phys.* **60** 701
[2] Mills A P Jr 1995 *Positron and positronium emission spectroscopies* , in *Positron Spectroscopy of Solids*, Dupasquier A and Mills A P eds, (IOS, Amsterdam) p. 209
[3] Brusa R S and Dupasquier A 2010 *Positronium emission and cooling*, in *Physics with many Positrons*, Dupasquier A, Mills A P jr and Brusa R S eds, (North Holland, Amsterdam) p 245
[4] Cassidy D B 2010 *Experiment with many-positron system*, in *Physics with many Positrons*, Dupasquier A, Mills A P jr and Brusa R S eds, (North Holland, Amsterdam) p. 1
[5] Cassidy D B and Mills A P jr 2011 *Phys. Rev. Lett.* **107** 213401
[6] Mills A. P. Jr 2010 *Physics with many Positrons*, in *Physics with many Positrons*, Dupasquier A, Mills A P jr and Brusa R S eds, (North Holland, Amsterdam) p. 77
[7] Cassidy D B, Hisakado T H, Tom H W K and Mills A P jr 2012 *Phys. Rev. Lett.* **108** 133402
[8] Cassidy D B, Hisakado T H, Tom H W K and Mills A P jr 2012 *Phys Rev. Lett.* **108** 043401
[9] Kellerbauer A *et al.*2008 *Nucl. Instrum. Methods Phys. Res.* ***B*** **266** 351
[10] Mariazzi S. et al. 2013 *Nucl. Instrum. Methods Phys. Res. B, submitted*
[11] Mariazzi S, Brusa R S 2011 *J. Phys. : Conf. Series* **262** 012037
[12] Pedersen T S, Danielson J R, Hugenschmidt C, Marx G, Sarasola X, Schauer F, Schweikhard L, Surko C M 2012 *New Journal of Physics* **14** 035010
[13] Mills A P Jr and Leventhal M 2002 *Nucl. Instrum. Methods Phys. Res.* ***B*** **192** 102
[14] Cassidy D B, Hisakado T H, Tom H W K and Mills A P jr 2011 *Phys. Rev. Lett.* **106** 133401
[15] Mariazzi S, Salemi A and Brusa R S 2008 *Phys. Rev. B* **78** 085428
[16] Mazzoldi P, Mattei G, Ravelli L, Egger W, Mariazzi S and Brusa R S 2009 *J. Phys. D: Appl. Phys.* **42** 115418
[17] Nagashima Y, Morinaka Y, Kurihara T, Nagai Y, Hyodo T, Shidara T and Nakara K 1998 *Phys. Rev. B*, **58** 12676
[18] Mariazzi S, Bettotti P, Larcheri S, Toniutti L and Brusa R S 2010 *Phys. Rev. B* **81** 235418
[19] Mariazzi S, Di Noto L, Ravelli L, Egger W, Brusa R S 2013 Journ. of Phys. Conference Series **443** 012061
[20] Mariazzi S, Bettotti P and Brusa R S 2010 *Phys. Rev. Lett.* **104** 243401
[21] Pantel N, Mariazzi S, Toniutti L, Checchetto R, Miotello A, Dirè S and Brusa R S 2007 *J. Phys. D: Appl. Phys.* **40** 5266-5274
[22] He C., Ohdaira T., Oshima N., Muramatsu M., Kinomura A., Suzuki R., Oka T. and Kobayashi, Y. 2007 *Phys. Rev. B* **75** 195404
[23] Cassidy D B, Crivelli P, Hisakado T H, Liszkay L, Meligne V E, Perez P, Tom H W K and Mills A P Jr. 2010 *Phys. Rev.* ***A*** **81** 012715
[24] Zecca A, Bettonte M, Paridaens J, Karwasz G P and Brusa R S 1998 Meas. Sci. Technol. **9** 409
[25] Egger W 2010 *Pulsed low-energy positron beams in material sciences*, W. Egger in *Physics with many Positrons*, ed. by Dupasquier A, Mills A P jr and Brusa R S eds, (North Holland, Amsterdam) p 419
[26] Hugenschmidt C 2010 *Positron sources and positron beams*, in *Physics with many Positrons* Dupasquier A, Mills A P jr and Brusa R S eds, (North Holland, Amsterdam) p 399
[27] Di Noto L, Mariazzi S, Bettonte M, Nebbia G and Brusa R S 2012 *Eur. Phys. J. D* **66** 118
[28] Brusa R S, Macchi C, Mariazzi S, Karwasz G P, Egger W, Sperr P and G. Kögel G 2005 P*hys. Rev. B* **71** 245320
[29] Cassidy D B, Hisakado T H, Meligne V E, Tom H W K, Mills A P jr. 2010 *Phys. Rev.* ***A*** **82** 052511
[30] Sauder W C 1968 *J. Res. Natl. Bur. Stand. A* **72** 91
[31] Nagashima Y et al. 1995 *Phys. Rev. A* **52** 258